Nanoscale

Accepted Manuscript

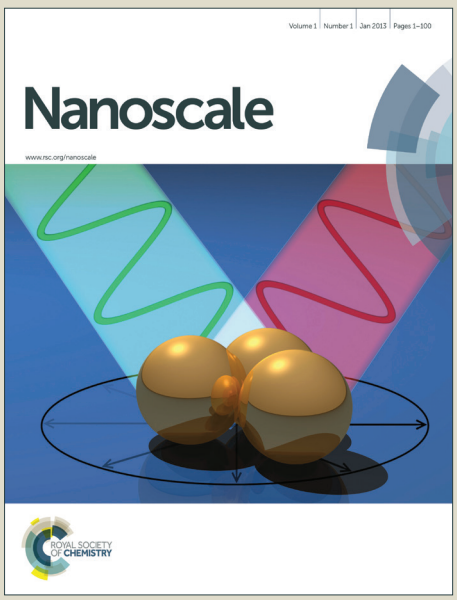

ROYAL SOCIETY OF CHEMISTRY

www.rsc.org/nanoscale

Journal Name

RSCPublishing

ARTICLE

Bacteriophage-based Nanoprobes for Rapid Bacteria Separation

Juhong Chen,[a] Bradley Duncan,[b] Li-Sheng Wang,[b] Vincent M. Rotello*[b] and Sam R. Nugen*[a]

Cite this: DOI: 10.1039/x0xx00000x

Received ooth January 2012,
Accepted ooth January 2012

DOI: 10.1039/x0xx00000x

www.rsc.org/

The lack of practical methods for bacterial separation remains a hindrance for the low-cost and successful development of rapid detection methods from complex samples. Antibody-tagged magnetic particles are commonly used to pull analytes from a liquid sample. While this method is well-established, improvements in capture efficiencies would result in an increase of the overall detection assay performance. Bacteriophages represent a low-cost and more consistent biorecognition element as compared to antibodies. We have developed nanoscale bacteriophage-tagged magnetic probes, where T7 bacteriophages were bound to magnetic nanoparticles. The nanoprobe allowed the specific recognition and attachment to *E. coli* cells. The phage magnetic nanprobes were directly compared to antibody-conjugated magnetic nanoprobes. The capture efficiencies of bacteriophages and antibodies on nanoparticles for the separation of *E. coli* K12 at varying concentrations were determined. The results indicated a similar bacteria capture efficiency between the two nanoprobes.

Introduction

Advances in rapid bacteria detection methods have enabled improvements in speed, sensitivity and specificity in fields such as medical diagnostics, biowarfare detection, food safety, water quality and environmental monitoring. Technologies such as surface plasmon resonance (SPR)[1], surface enhanced Raman scattering (SERS)[2], electrochemical detection,[3, 4] field effect transistor biosensors (FET) and quartz crystal microbalance (QCM)[5, 6] are examples of emerging detection methods, which require a relatively clean sample in a small volume to achieve enhanced sensitivity. Unfortunately, such methods typically require a significant sample purification or preparation step prior to analysis. Analysis of complex samples (containing non-target lipids, proteins, carbohydrates, inhibitors, or other interferents) remains a unique challenge to utilizing such high sensitivity detection methods. Stevens and Jaykus suggested that an ideal separation method should 1) separate the analyte from the sample, 2) remove any possible inhibitors to a downstream detection system, and 3) reduce the sample size while maintaining a high capture efficiency of bacteria.[7]

Immunomagnetic separation (IMS) is a common separation method in which magnetic beads tagged with analyte-specific antibodies are incubated with the analyte. When a magnet is placed near the sample tube, the beads (on which the analyte is bound) are pulled toward the magnet and the remaining liquid sample can be aspirated. IMS beads (typically 1-5 µm in diameter, onto which antibodies for a range of bacterial analytes are conjugated) are commercially available from several companies. While this method is widely used, improvements to the capture efficiencies and cost would allow the method to become more utilized. Recently, magnetic nanoparticles (MNPs) have attracted attention in various fields such as biomedicine, drug delivery, and diagnostics due to their unique magnetic properties.[8-10] Magnetic nanoparticles have been reported to efficiently separate *E. coli* O157:H7 in ground beef[11, 12] and *Listeria monocytogenes* from both nutrient broth and milk samples[13]. Unfortunately, traditional iron oxide nanoparticles require extended periods of time to separate due to slow particle velocities.

Bacteriophages, also known simply as phages, are viruses which infect specific bacterial cells. Phages have the ability to very strongly and specifically bind to target bacteria.[14, 15] They are able to recognize a bacterium, infect it, and lyse it releasing hundreds to thousands of replicated phages in the process. Detecting bacteria using engineered phages by fluorescent labeling of phage nucleic acid[16] and phage components[17], phage-integrated colorimetric, fluorescent, and bioluminescent reporter genes[18] and phage-integrated green fluorescent protein[19] has shown promising results.

The use of antibodies for separation can result in inconsistencies due to batch to batch variations. The relatively high cost of antibodies has led to research towards alternative biorecognition elements such as aptamers.[20, 21] Unlike antibodies and aptamers, phages are relatively easy and inexpensive to synthesize and purify. Due to the extremely strong binding affinity,[22] phage have recently been used as low-cost biorecognition elements for bacteria.[15, 23] The host range of bacteriophages can be either extremely wide or narrow allowing for isolation of an entire genus or species.[24] The phages are also more stable than antibodies with regards to temperature, pH and ionic strength.[25]

The challenge in using infective bacteriophages as recognition elements for separation lies in the infection cycle of the

particular phage. The complete infection cycle can last as little as 25 minutes and results in lysed bacteria. Although this could be ideal for downstream genetic analysis such as PCR, if the bacteria have not been separated from the sample solution before cell lysis, the process would fail. Therefore the combination of bacteriophages and magnetic nanoparticles would require separation speeds much faster than those offered by iron oxide nanoparticles which require a significant separation time.

In this paper, we have bound T7 bacteriophage on magnetic nanoparticles for the purpose of separating *E. coli* from a liquid solution. For the nanoparticles, mixed metal oxide (FeCo) magnetic nanoparticles containing 30% cobalt (w/w) were used as core materials. The cobalt allowed improved separation velocities as compared to iron oxide. The magnetic nanoparticles were coated with a silica shell, onto which streptavidin was immobilized for subsequent conjugation of biotinylated T7 bacteriophage and antibodies. The nanoscale phage magnetic probes were used to separate *E. coli* K12 at concentrations ranging from 10^2 to 10^7 CFU mL^{-1}.

Results and discussion

Preparation and characterization of FeCo MNPs

The challenge for using single domain MNPs in magnetic applications is the inherent aggregation which occurs even without an external magnetic field. However, superparamagnetic nanoparticles[26] such as Fe_3O_4, γ-Fe_2O_3, cobalt oxides and mixed metal oxides (without inter-particle magnetic attractive forces) have been utilized in biomedicine, drug delivery and cancer research.[27, 28] Karimi *et al.* reported that 7 nm FeCo MNPs have the highest saturation magnetization compared to the other MNPs with the same size.[27] Mixed metal oxide FeCo MNPs were therefore utilized as core materials for our study.

Monodisperse FeCo MNPs capped with oleic acid were synthesized using previously reported procedures.[29, 30] Briefly, surfactants were used to surround the iron and cobalt salts resulted in the formation of the initial monomers. When the supersaturated monomers were heated, they became a nucleation site for particle growth. Once cooled, the nanoparticles were able to be dispersed in a non-polar solvent such as hexane due to the hydrocarbon tail of the oleic acid cap. The size of FeCo magnetic nanoparticles was found to be 9.1 ± 2.3 nm in diameter (Fig. 1a). In order to determine the magnetic behavior of FeCo MNPs, the magnetic hysteresis loops were performed at room temperature (T = 300 K) using a superconduction quantum interference device (SQUID). The FeCo MNPs were found to be superparamagnetic with zero coercivity. The saturated magnetization value of FeCo MNPs at room temperature was appropriately 59 emu g^{-1} (Fig. 1b), which was similar to previously reported value.[30] The X-ray photoelectron spectroscopy (XPS) analysis of MNPs was shown in -1, indicating the present of Fe (727 eV) and cobalt (787 eV). The FeCo MNPs were able to be separated from hexane with an external magnetic field. Following removal of the magnetic field, the particles were able to be redisbursed with mild agitation.

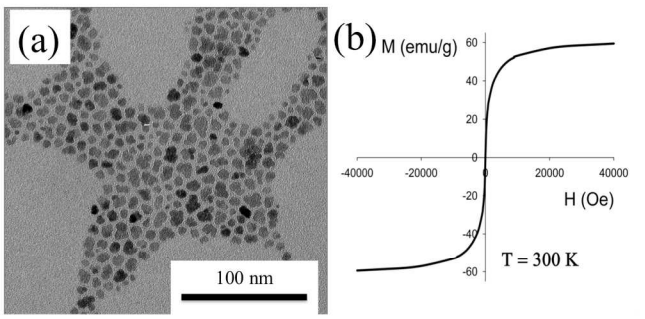

Fig. 1 a) Transmission Electron Microscopy (TEM) image of oleic acid protected FeCo MNPs, and b) magnetization curve of FeCo MNPs at room temperature.

Immobilization of streptavidin on FeCo MNPs

The steps to immobilize streptavidin on FeCo MNPs are shown in Fig 2a. In order to protect the mental core from the sample matrix, the FeCo MNPs were first coated with a silica shell[31] which also served as a more suitable and convenient functionalizable surface. In this study, we prepared the silica-coated FeCo MNPs using a reverse microemulsion in cyclohexane. A non-ionic surfactant (Igepal® CO-520) was used to suspend the oleic acid-covered FeCo MNPs in aqueous $NH_3 \cdot H_2O$. The surfactant allowed the formation of a water layer on the nanoparticles for hydrolysis of TEOS. The optimal ratio of Igepal® CO-520 to $NH_3 \cdot H_2O$ minimized the number of micelles which contained multiple FeCo nanoparticles in the core. The thickness of silica shell has previously been reported to be tunable from 2 nm to 100 nm.[32] The thickness of silica layers on FeCo MNPs which were used for this study was 9.0 ± 1.8 nm (Fig. 2b). The present of silica shell was also confirmed using XPS analysis (Fig. S1). The TEM image of streptavidin

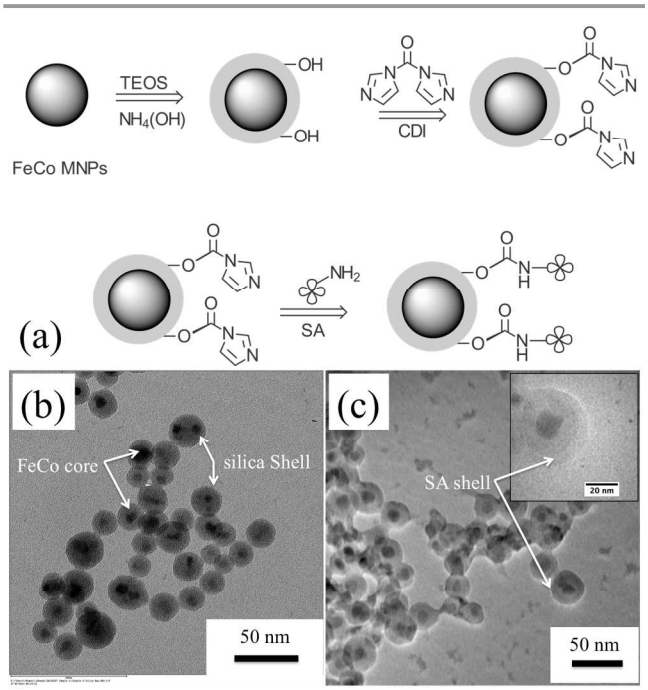

Fig. 2 Functionalization magnetic nanoparticles. a) A silica shell was synthesized from tetraethylorthosilicate (TEOS) which was then functionalized with streptavidin (SA) using carbonyldiimidazole (CDI). b) Transmission electron micrographs of silica-coated FeCo MNPs. c) TEM images of streptavidin coated on MNPs (insets: streptavidin coated on MNPs at high magnification).

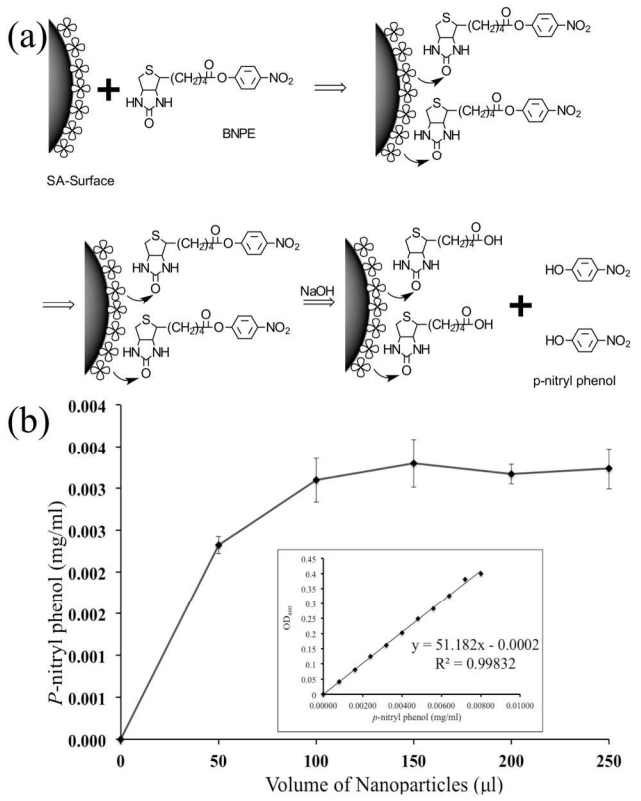

Fig. 3 a) Schematic showing the mechanism to measure the biotin binding capacity and b) biotin binding capacity of streptavidin-coated nanoparticles.

coated on FeCo MNPs is shown in Fig. 2c. A thin layer of streptavidin can be identified on the surface of the MNPs.

This silica layer has the following advantages: 1) it allows convenient conjugation chemistries; 2) it provides a separation of the magnetic cores and reduces aggregation and 3) it decreases non-specific absorption of biological species.[33]

A common method used to immobilize proteins on the surface of nanoparticles is by covalent attachment using 3-aminopropyltriethoxysilane (APTES) and glutaraldehyde.[34] However, Gopinath et al. compared several methods of surface modification and concluded that *N, N'*-Carbonyldiimidazole (CDI) provided an improved direct immobilization of molecules without an intermediate chemical linker.[35] The method used to immobilize streptavidin on silica-coated FeCo MNPs in this study was shown in Fig. 2a. The CDI was used to activate the silanol group on the surface of silica shell promoting conjugation to a primary amine on the streptavidin protein.

Determination of biotin binding capacity of nanoparticles

In this study, these nanoparticles were functionalized with streptavidin for the attachment of a biorecognition element (phages or antibodies). In order to fully cover nanoparticles with phages and antibodies, the biotin binding capacities on these nanoparticles were determined. Therefore, the total concentration of biorecognition elements was comparable across all treatments. A colorimetric measurement was performed to determine the biotin binding capacity of streptavidin on the nanoparticle. A solution of *d*-biotin *p*-nitrophenyl ester (BNPE) was reacted with nanoparticle solutions of varying immobilized streptavidin in the biotin

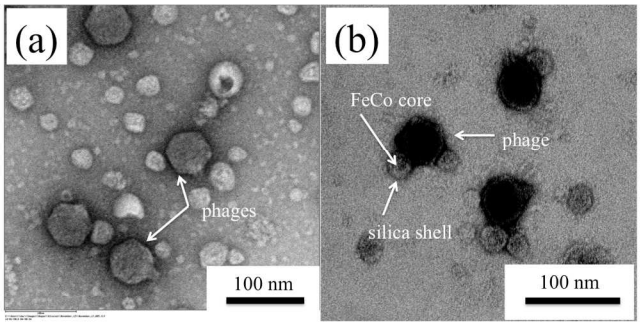

Fig. 4 TEM images of a) negative uranyl acetate staining of biotin T7 phage and b) positive uranyl acetate staining of biotin T7 phage attached to streptavidin-coated FeCo MNPs.

binding sites. Following incubation, the magnetic nanoparticles were washed three times to remove unbound NBPE. In the present of NaOH, the bound BNPE was hydrolyzed to produce *p*-nitryl phenol (yellow), which was quantified at 400 nm (Fig. 3a).[36] The absorbance values of nanoparticles were compared to a standard curve (R^2 = 0.998) of *p*-nitryl phenol (Fig. 3b). Finally, the biotin binding capacity of streptavidin on magnetic nanoparticles was calculated using equation 1:

$$C = \frac{cV}{\mathrm{MW} \times m} \times 10^9 \qquad (1)$$

In the above equation, C (nmol mg^{-1}) refers to the biotin binding capacity of streptavidin-coated magnetic nanoparticles, c was the concentration of *p*-nitryl phenol (mg mL^{-1}), V is the volume of hydrolyzed supernatant solution, MW is the molecule weight of *p*-nitryl phenol (g mol^{-1}) and m is the weight of streptavidin-coated magnetic nanoparticles.[36] The biotin binding capacity of streptavidin-coated nanoparticles is 166.95 ± 12.87 nmol mg^{-1}. This represented approximately 8 × 10^3 biotin binding sites per nanoparticle.

Biofunctionalization of nanoparticles with phages or antibodies

In this study, antibodies modified with biotin were conjugated to streptavidin-coated magnetic nanoparticles. The TEM image of negative uranyl acetate stained biotin-modified T7 phage without nanoparticles was shown in Fig. 4a. Similarly, T7 bacteriophages, which were genetically engineered to express biotin on the capsid[37] was able to directly bind with streptavidin magnetic nanoparticles (Fig. 4b). Following standardization of

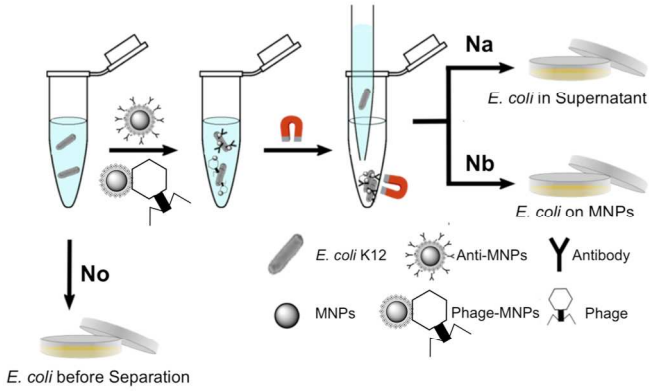

Fig. 5 Magnetic separation of bound bacteria on the magnetic nanoprobes from unbound bacteria in the supernatant (not drawn to scale).

the biotin binding capacity of nanoparticles, the number of phages conjugated on nanoparticles was enumerated following standard plaque assay procedure, resulting in (1.50 ± 0.53) × 10^{10} PFU mg^{-1}. Based on eleven TEM images, the phage-MNPs complex was counted and one phage per magnetic nanoparticle accounted for 74% of all phage-MNPs complexes. Phages bounded with two or three nanoparticles were also found (Fig. 4b).

Comparison of the capture efficiency between antibody and phage-conjugated magnetic nanoprobes

Typical IMS beads conjugated to antibodies for specific bacteria are commercially available from several companies.[38, 39] By using nano-scale particles, the capture efficiency is increased. When used to capture E. coli O157:H7 in ground beef, a capture efficiency of over 90% was achieved.[11] Similar results were found by Pappert *et al.* who calculated a 96 ± 6% capture efficiency of *E. coli* from a 10^6 CFU ml^{-1} culture.[12] In this study, the two magnetic nanoprobes (T7 phages and antibodies on magnetic nanoparticles) were used to separate *E. coli* K12 (range: 10^2 to 10^7 CFU mL^{-1}) from 1 mL sample solution. Nanoparticles utilizing an antibody capture were incubated with the bacteria using standard protocols of 30 minutes with mild agitation. A shortened binding time was required for the T7 phages containing particles as 30 minutes could have resulted in lysis of bacteria. Therefore, the phage nanoparticles were incubated for only 15 minutes prior to magnetic separation. Following hybridization, all nanoparticle variants were rapidly separated using an external magnet (Fig. 5). The capture efficiency was calculated using the equations 2 and 3:

$$CE_1\ (\%) = \left(1 - \frac{N_a}{N_o}\right) \times 100\% \quad (2)$$

$$CE_2\ (\%) = \frac{N_b}{N_o} \times 100\% \quad (3)$$

Where, N_o is the total number of *E. coli* K12 cells present in the initial sample (CFU), N_a is the number of *E. coli* K12 cells which remained unbound to the particles (CFU), N_b is the number of *E. coli* K12 cells bound to the particles (CFU).[11] Due to aggregation of the separated nanoparticle/bacteria complex, quantification using standard plating methods made CE_2 (Equation 3) unreliable. This phenomenon has previously been reported with the magnetic separation of *E. coli*.[11, 13] Therefore, the capture efficiency was reported using CE_1 (Equation 2).

The separated nanoparticles and bacteria were imaged using transmission electron microscopy (TEM) (Fig. 6a,b). The TEM images of bacteria were shown in Fig. S3. The capture efficiency (CE_1) of the two magnetic nanoprobes can be seen in Figure 6c. In order to determine the specific bind between the nanoprobes and *E. coli* cell, the negative control result of streptavidin coated MNPs was shown (Fig. S4). A similar capture efficiency between phage and antibody magnetic nanoprobes was obtained, indicating that phages produced easily and at low cost can replaced the commonly used antibodies for bacteria separation at nanoscale size.

In order to further confirm that phages can be used as biorecognition elements for bacteria separation instead of antibodies, magnetic beads at microscale size was measured. The commercial streptavidin-coated magnetic microbeads modified with phages and antibodies were used to separate *E. coli* K12. Firstly, the biotin binding capacity of streptavidin-coated magnetic microbeads was measured using above-mentioned method and 306.54 ± 26.04 nmol mg^{-1} (Fig. S2). In order to equal the biotin binding capacity at micro and nanoscale size, the amount of streptavidin-coated microbeads was normalized. Next, phages and antibodies were immobilized on these microbeads for bacterial separation. The TEM images of microbeads and bacteria were shown in Fig. S5a-b. Compared with antibody magnetic microprobe, phage magnetic microprobe resulted in a higher capture efficiency (Fig. S5c). Among all magnetic probes, the lowest capture efficiency was the current standard for IMS which used antibodies on microbeads. Phage-conjugated magnetic probe showed a promising tool for bacteria separation.

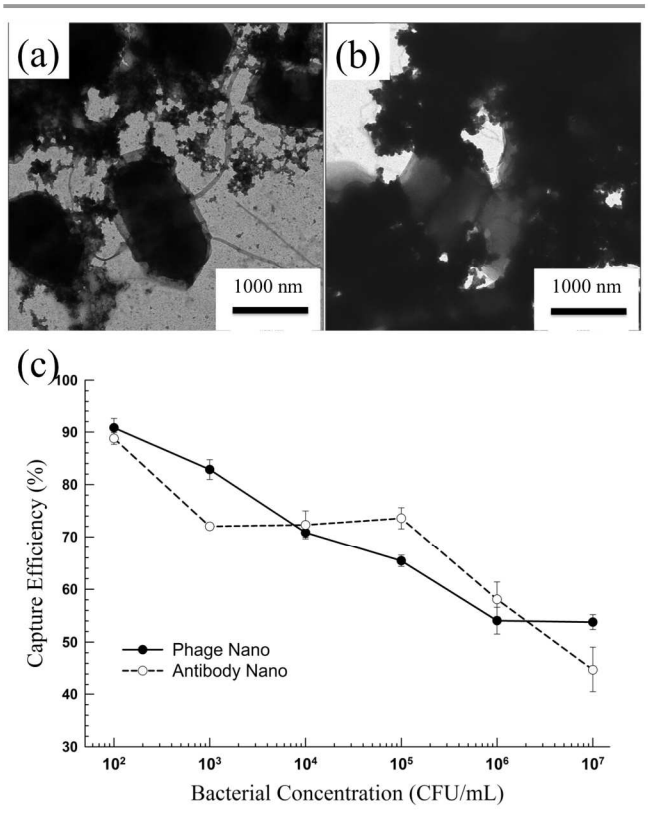

Fig. 6 TEM images of nanoprobes bound to *E. coli* K12: a) antibody-conjugated nanoparticles and b) phage-conjugated nanoparticles, c) comparison the capture efficiency between the two magnetic nanoprobes: phage magnetic nanoprobes (solid round line) and antibody magnetic nanoprobes (hollow round line).

Conclusions

We have developed nanoscale T7 bacteriophage magnetic nanoprobes for the low-cost and efficient separation of bacteria from liquid sample. The capture efficiency at all bacterial concentrations (10^2-10^7 CFU mL^{-1}) was not significantly different between the bacteriophage magnetic nanoparticles and antibody magnetic nanoparticle while using only half the incubation time for phage magnetic probes. Compared with traditional filtration, the key feature using magnetic nanoparticles modified as biorecognize elements is that they can specifically concentrate and separate target bacteria cell. It should also be noted that the application of phages as a detection nanoprobes provides many advantages over other molecular probes due to their relative ease of production, host specificity, ability to distinguish between viable and non-viable cells, and potential for rapid bacteria detection. Additionally,

phages are highly stable to temperature, pH variations, organic solvents and degradation by proteases.[40]

While most detection devices require small and relatively clean samples, many sample matrices such as food, soil and feces are inherently complex and contain inhibitors for downstream analytical tools such as PCR. In these cases, a sample preparation step becomes a necessary tool for reliable testing. Additionally, many organisms such as *Listeria monocytogenes*, *Salmonella* spp. and *E. coli* O157:H7 have a zero tolerance in food thus requiring the ability to detect a single organism in a 25 gram sample. While typical protocols require an enrichment step to grow the organisms, this process takes hours to days and is therefore not suitable to all sample types such as fresh produce. Bacteriophages on magnetic nanoparticles represents an improved separation/concentration tool as compared to the current molecular biology standard, IMS.

In order to eliminate the infectivity of toxicity of bacteriophage for bacteria separation, further studies will focus on conjugating ghost phage (able to bind, but not infect) on nanoparticles to better quantification of the separation ability for target bacterial detection.[41] This will allow a fast and low-cost method to isolate and detect bacteria. Additionally, the separated bacteria would also undergo a natural lysis as part of the infection. This can allow access to the DNA for applications such as QPCR and therefore allow the determination of only viable organisms as infection would not occur in nonviable bacteria.

Materials and methods

Synthesis of oleic acid protected FeCo MNPs

The oleic acid protected FeCo MNPs were synthesised according to reported methods with some modifications.[29, 30] $Fe(acac)_3$ (1 mmol, 0.3680 g), $Co(acac)_2$ (2 mmol, 0.5355 g), and 1,2-hexadecanediol (3 mmol, 0.9675 g) were placed into a three-neck round bottomed reaction flask with dibenzyl ether (50.0 mL). The reaction mixture was stirred for 30 minutes under flowing nitrogen gas to allow the removal of air. The mixture was then slowly heated to 100 °C and kept at this temperature for 10 minutes. The surfactants, oleylamine (4.25 mL) and oleic acid (4.00 mL) were added into reaction flask and the reaction mixture was then heated to 200 °C for 20 minutes. Following the brief incubation, the reaction mixture was heated to reflux (~300 °C) for 60 minutes. During this process, the solution color changed from purple to black, indicating the formation of FeCo MNPs. The black solution was then cooled down to room temperature and the particles were precipitated using ethanol (20 mL) with centrifugation at 7500 x g for 10 minutes. The particles were then washed three times with a mixture of ethanol and hexane (3:1, V/V). Finally, the FeCo MNPs were dispersed in hexane until use.

Preparation of silica-coated FeCo core/shell MNPs

The silica-coated FeCo core/shell MNPs were prepared using a modification of a previously reported method.[42] Polyoxyethylene(5)nonylphenyl ether (7 mmol, 3.0 g, Igepal CO-520) was dispersed in cyclohexane (50.0 mL). Next, dried FeCo MNPs (10 mg) were transferred into cyclohexane (5.0 mL) and briefly sonicated. The two cyclohexane solutions were mixed until a clear solution formed. Ammonium hydroxide (25%, 0.5 mL) was added to form a clear brown reverse microemulsion. Lastly, tetraethylorthosilicate (30 μL, TEOS) was added, and gently agitated for 48 hours at room temperature. Methanol was added into the solution to remove the excess surfactant and the silica-coated FeCo core/shell MNPs were precipitated and washed three times using sonication and centrifugation with mixture of ethanol and hexane (1:3, V/V). The particles were then redispersed in ethanol until use.

Immobilization of streptavidin on silica-coated FeCo MNPs[43]

The silica-coated FeCo MNPs (10 mg) were placed into a scintillation vial and washed sequentially with 5 mL each of a mixture of DI water and dimethyl sulfoxide (DMSO) (3:7, 5:5, 7:3, V/V). The particles were then washed three times in anhydrous DMSO to minimize the water content. *N, N'*-Carbonyldiimidazole (1.0 mL, 10 mg mL^{-1}, CDI in DMSO) was then added into the scintillation vial. Next, the vial was agitated for 2 hours at room temperature. The MNPs were then washed three times with anhydrous DMSO to remove excess CDI, and washed using ice-cold sodium phosphate buffer solution (0.01 M, pH 7.4, PBS: 10 mM Na_2HPO_4, 1.8 mM KH_2PO_4, 137 mM NaCl, 2.7 mM KCl). The MNPs were redispersed in PBS (5 mL, 0.01 M, pH 7.4), and streptavidin (500 μL, 1 mg mL^{-1} in PBS) was then added to the mixture. The conjugation solution was agitated for 12 hours at room temperature. Following conjugation, the MNPs were washed three times with PBS (0.01 mM, pH 7.4) using magnetic separation and stored at 4 °C.

Quantification of biotin binding capacity of streptavidin coated nanoparticles[36]

Several volumes of streptavidin-coated nanoparticles solution (0, 50, 100, 150, 200, 250 μL, 2 mg mL^{-1}) were washed three times with acetate buffer (1 mL, 0.2 M, pH 5.0, 166 mM sodium acetate trihydrate, 34 mM glacial acetic acid, 0.05% Tween 20), and finally dispersed in acetate buffer (1mL, 0.2 M). Following washing, *d*-biotin *p*-nitrophenyl ester (100 μL, 10 mg mL^{-1} in DMSO, BNPE) was added and incubated for 30 minutes with gentle agitation. The nanoparticles were then washed five times with above acetate buffer (1 mL, 0.2 M) to remove excess BNPE and finally dispersed in NaOH solution (1 mL, 0.1 M). The BNPE bound to nanoparticles hydrolyzed and produced *p*-nitryl phenol (yellow) which was quantified at 400 nm.

Preparation of biotinlyted T7 bacteriophage

T7 bacteriophage was previously genetically modified to express the 15 AA (GLNDIFEAQKIEWHE) biotin ligase (BirA) target on the capsid.[44] The endogenous BirA within *E. coli* was able to conjugate biotin molecules to the phage capsid during replication. *E. coli* BL21 was grown overnight in Luria-Bertani (LB) broth (50 mL, pH 7.4, 10 g L^{-1} tryptone, 5 g L^{-1} yeast extract, 10 g L^{-1} NaCl) at 250 rpm (37 °C). Following the overnight growth, the culture was reinoculated into fresh LB broth (35 mL), and agitated at 250 rpm for 3 hours at 37 °C. After the OD_{600} of the culture reached 0.6–0.8, a high titer biotin T7 phage lysate (5 μL, 10^{10} CFU mL^{-1}) was added and the culture was again incubated for 1 hour at 37 °C until the solution cleared. Following the addition of salt (3 mL, 5 M NaCl), the culture was centrifuged at 7000 rpm for 10 minutes at 4 °C. The supernatant was stored at 4 °C until use.

Preparation of antibody or phage magnetic nanoprobes

Biotin-modified anti-*E. coli* K12 antibodies (10 μL, 4 mg mL^{-1}) or biotinlyated T7 phage (1 mL, 3.5×10^{10} CFU mL^{-1}) were tagged onto streptavidin-coated nanoparticles (1 mL, 1.8 mg $mL^{-1)}$. The solutions were incubated for 30 minutes with gentle agitation at room temperature. All nanoparticles were washed a minimum of three times with above PBS (0.01 M, pH 7.4) to remove unbound antibodies or phages. The nanoparticles were dispersed in PBS (1 mL, 0.01M, pH 7.4) and stored at 4 °C until use.

Estimation of the capture efficiency of phage or antibody probes on bacterial separation

E. coli K12 was inoculated into above LB broth (50 mL) and rotated at 250 rpm overnight at 37 °C. Antibody magnetic nanoparticles (100 μL, 1.8 mg mL^{-1}) and phage magnetic nanoparticles (100 μL, 1.8 mg mL^{-1}) were added into bacterial samples (1 mL, *E. coli* K12) in PBS (0.01 M, pH 7.4) with a range of concentrations (102-107 CFU mL^{-1}). The mixtures were incubated 30 minutes for antibody magnetic probes and 15 minutes for phage magnetic probes at 10 rpm at room temperature. The magnetic probes for *E. coli* K12 were separated and washed three times with PBS (0.01M, pH 7.4) by magnetic separation. The concentrations of *E. coli* in the original solution, *E. coli* (phage) in supernatant solution and *E. coli* (phage) on magnetic probes were counted using serial dilutions on LB plates (pH 7.4, 10 g L^{-1} tryptone, 5 g L^{-1} yeast extract, 10 g L^{-1} NaCl, 15 g L^{-1} agar).

Acknowledgements

We thank the USDA 2013-02037 for supporting this research financially. Dale A. Callaham is acknowledged for his assistance with the TEM imaging. This work is supported in part by the Nanoscale Science and Engineering Initiative of the National Science Foundation under NSF Award Number CMMI-1025020. Additional thanks go to Professor Mark Tuominen in the Department of Physics at the University of Massachusetts, Amherst for the use of his SQUID magnetometer. The authors would like to thank Dr. Sankar Adhya at the national Cancer Institute for the modified T7 bacteriophage.

Notes and references

[a] Department of Food Science, University of Massachusetts, Amherst, 102 Holdsworth Way, Amherst, Massachusetts, 01003, USA. E-mail: snugen@umass.edu

[b] Department of Chemistry, University of Massachusetts, Amherst, 710 North Pleasant Street, Amherst, Massachusetts, 01003, USA.

E-mail: rotello@chem.umass.edu

† Footnotes should appear here. These might include comments relevant to but not central to the matter under discussion, limited experimental and spectral data, and crystallographic data.

Electronic Supplementary Information (ESI) available: [details of any supplementary information available should be included here]. See DOI: 10.1039/b000000x/

1. N. Tawil, E. Sacher, R. Mandeville and M. Meunier, *Biosens. Bioelectron.*, 2012, **37**, 24-29.
2. C. Fan, Z. Q. Hu, A. Mustapha and M. S. Lin, *Appl. Microbiol. Biotechnol.*, 2011, **92**, 1053-1061.
3. J. Chen, Z. Jiang, J. D. Ackerman, M. Yazdani, S. Hou, S. R. Nugen and V. M. Rotello, *Analyst*, 2015, **140**, 4991-4996.
4. M. R. Akanda, V. Tamilavan, S. Park, K. Jo, M. H. Hyun and H. Yang, *Anal. Chem.*, 2013, **85**, 1631-1636.
5. Z. Shen, M. Huang, C. Xiao, Y. Zhang, X. Zeng and P. G. Wang, *Anal. Chem.*, 2007, **79**, 2312-2319.
6. K. Zhang, L. Fu, L. Zhang, Z. Y. Cheng and T. S. Huang, *Biotechnol. Bioeng.*, 2014, **111**, 2229-2238.
7. K. A. Stevens and L. A. Jaykus, *Crit. Rev. Microbiol.*, 2004, **30**, 7-24.
8. M. A. Nash, J. N. Waitumbi, A. S. Hoffman, P. Yager and P. S. Stayton, *ACS Nano*, 2012, **6**, 6776-6785.
9. N. A. Frey, S. Peng, K. Cheng and S. H. Sun, *Chem. Soc. Rev.*, 2009, **38**, 2532-2542.
10. J. Xie, C. Xu, N. Kohler, Y. Hou and S. Sun, *Adv. Mater.*, 2007, **19**, 3163-3166.
11. M. Varshney, L. J. Yang, X. L. Su and Y. B. Li, *J. Food Prot.*, 2005, **68**, 1804-1811.
12. G. Pappert, M. Rieger, R. Niessner and M. Seidel, *Microchimica Acta*, 2010, **168**, 1-8.
13. H. Yang, L. Qu, A. N. Wimbrow, X. Jiang and Y. Sun, *Int. J. Food Microbiol.*, 2007, **118**, 132-138.
14. S. A. Soper, A. C. Henry, B. Vaidya, M. Galloway, M. Wabuyele and R. L. McCarley, *Anal. Chim. Acta*, 2002, **470**, 87-99.
15. H. Handa, S. Gurczynski, M. P. Jackson, G. Auner, J. Walker and G. Mao, *Surf. Sci.*, 2008, **602**, 1392-1400.
16. L. Goodridge, J. Chen and M. Griffiths, *Appl. Environ. Microbiol.*, 1999, **65**, 1397-1404.
17. A. Singh, S. K. Arya, N. Glass, P. Hanifi-Moghaddam, R. Naidoo, C. M. Szymanski, J. Tanha and S. Evoy, *Biosens. Bioelectron.*, 2010, **26**, 131-138.
18. A. E. Smartt, T. Xu, P. Jegier, J. J. Carswell, S. A. Blount, G. S. Sayler and S. Ripp, *Anal. Bioanal. Chem.*, 2012, **402**, 3127-3146.
19. S. H. Lee, M. Onuki, H. Satoh and T. Mino, *Lett. Appl. Microbiol.*, 2006, **42**, 259-264.
20. S. J. Wu, N. Duan, Z. P. Wang and H. X. Wang, *Analyst*, 2011, **136**, 2306-2314.
21. S. Wang, A. K. Singh, D. Senapati, A. Neely, H. Yu and P. C. Ray, *Chemistry-a European Journal*, 2010, **16**, 5600-5606.
22. R. Moldovan, E. Chapman-McQuiston and X. Wu, *Biophys. J.*, 2007, **93**, 303-315.
23. V. Nanduri, I. B. Sorokulova, A. M. Samoylov, A. L. Simonian, V. A. Petrenko and V. Vodyanoy, *Biosens. Bioelectron.*, 2007, **22**, 986-992.
24. L. Bielke, S. Higgins, A. Donoghue, D. Donoghue and B. M. Hargis, *Poult. Sci.*, 2007, **86**, 2536-2540.
25. O. Minikh, M. Tolba, L. Brovko and M. Griffiths, *J. Microbiol. Methods*, 2010, **82**, 177-183.
26. Q. Dai, M. Lam, S. Swanson, R. H. R. Yu, D. J. Milliron, T. Topuria, P. O. Jubert and A. Nelson, *Langmuir*, 2010, **26**, 17546-17551.
27. T. D. Schladt, K. Schneider, H. Schild and W. Tremel, *Dalton Transactions*, 2011, **40**, 6315-6343.
28. C. Xu, B. Wang and S. Sun, *J. Am. Chem. Soc.*, 2009, **131**, 4216-4217.
29. G. S. Chaubey, C. Barcena, N. Poudyal, C. Rong, J. Gao, S. Sun and J. P. Liu, *J. Am. Chem. Soc.*, 2007, **129**, 7214-7215.
30. L. Hu, C. de Montferrand, Y. Lalatonne, L. Motte and A. Brioude, *Journal of Physical Chemistry C*, 2012, **116**, 4349-4355.
31. L. Chen, Z. Xu, H. Dai and S. Zhang, *J. Alloys Compd.*, 2010, **497**, 221-227.
32. M. Zhang, B. L. Cushing and C. J. O'Connor, *Nanotechnology*, 2008, **19**, 085601-085606.
33. S. A. Corr, Y. P. Rakovich and Y. K. Gun'ko, *Nanoscale Research Letters*, 2008, **3**, 87-104.
34. K. Can, M. Ozmen and M. Ersoz, *Colloids Surf. B. Biointerfaces*, 2009, **71**, 154-159.
35. S. C. B. Gopinath, K. Awazu, M. Fujimaki, K. Shimizu, W. Mizutani and K. Tsukagoshi, *Analyst*, 2012, **137**, 3520-3527.
36. F. Gao, B. F. Pan, W. M. Zheng, L. M. Ao and H. C. Gu, *J. Magn. Magn. Mater.*, 2005, **293**, 48-54.
37. T. K. Lu and J. J. Collins, *Proc. Natl. Acad. Sci.*, 2007, **104**, 11197-11202.

38. J. Chen, Y. Zhou, D. Wang, F. He, V. M. Rotello, K. R. Carter, J. J. Watkins and S. R. Nugen, *Lab Chip*, 2015, **15**, 3086-3094.
39. Z. Jiang, N. D. Le, A. Gupta and V. M. Rotello, *Chem. Soc. Rev.*, 2015, **44**, 4264-4274.
40. P. Schwind, H. Kramer, A. Kremser, U. Ramsberger and I. Rasched, *Eur. J. Biochem.*, 1992, **210**, 431-436.
41. C. M. Liu, S. H. Chung, Q. L. Jin, A. Sutton, F. N. Yan, A. Hoffmann, B. K. Kay, S. D. Bader, L. Makowski and L. H. Chen, *J. Magn. Magn. Mater.*, 2006, **302**, 47-51.
42. D. K. Yi, S. T. Selvan, S. S. Lee, G. C. Papaefthymiou, D. Kundaliya and J. Y. Ying, *J. Am. Chem. Soc.*, 2005, **127**, 4990-4991.
43. J. Ho, F. M. Al-Deen, A. Al-Abboodi, C. Selomulya, S. D. Xiang, M. Plebanski and G. M. Forde, *Colloids Surf. B. Biointerfaces*, 2011, **83**, 83-90.
44. R. Edgar, M. McKinstry, J. Hwang, A. B. Oppenheim, R. A. Fekete, G. Giulian, C. Merril, K. Nagashima and S. Adhya, *Proc. Natl. Acad. Sci. U. S. A.*, 2006, **103**, 4841-4845.